Infrared spectra and density functional theory calculations of the tantalum and niobium carbonyl dinitrogen complexes

Zhang-Hui Lu, Ling Jiang, and Qiang Xu

Citation: The Journal of Chemical Physics **131**, 034512 (2009); doi: 10.1063/1.3186759
View online: https://doi.org/10.1063/1.3186759
View Table of Contents: http://aip.scitation.org/toc/jcp/131/3
Published by the American Institute of Physics

Infrared spectra and density functional theory calculations of the tantalum and niobium carbonyl dinitrogen complexes

Zhang-Hui Lu,[1,2] Ling Jiang,[1] and Qiang Xu[1,2,a)]
[1]*National Institute of Advanced Industrial Science and Technology (AIST), Ikeda, Osaka 563-8577, Japan*
[2]*Graduate School of Engineering, Kobe University, Nada Ku, Kobe, Hyogo 657-8501, Japan*

(Received 28 May 2009; accepted 2 July 2009; published online 21 July 2009)

Laser-ablated tantalum and niobium atoms react with CO and N_2 mixtures in excess neon to produce carbonyl metal dinitrogen complexes, NN*M*CO (*M*=Ta, Nb), $(NN)_2$TaCO, and $NNTa(CO)_2$, as well as metal carbonyls and dinitrogen complexes. These carbonylmetal dinitrogen complexes are characterized using infrared spectroscopy on the basis of the results of the isotopic substitution and mixed isotopic splitting patterns. Density functional theory calculations have been performed on these novel species. The good agreement between the experimental and calculated vibrational frequencies, relative absorption intensities, and isotopic shifts supports the identification of these species from the matrix infrared spectra. Natural bond orbital analysis and plausible reaction mechanisms for the formation of the products are discussed. © *2009 American Institute of Physics*. [DOI: 10.1063/1.3186759]

I. INTRODUCTION

The interaction of transition-metal atoms with small molecules (i.e., CO, O_2, CO_2, H_2, N_2, CH_4, etc.) is of considerable interest in the widely different fields of catalysis, synthesis, and biology.[1] Among these small molecules, CO and N_2 are two of the most important in transition-metal chemistry from an academic or an industrial viewpoint.[1–5] Since the discovery of the first metal carbonyl $Ni(CO)_4$ and metal dinitrogen complex $[Ru(NH_3)_5(N_2)]^{2+}$,[6,7] the synthesis, structural characterization, and reactivity of transition-metal carbonyls and dinitrogen complexes have been the subject of intensive studies and are still important components of modern transition-metal chemistry. Compared to the extensive investigations on metal carbonyls or dinitrogen complexes,[8–10] few works have been done on carbonylmetal dinitrogen complexes. The first carbonyl dinitrogen complex, $(C_5H_5)Mn(CO)_2N_2$,[11] exhibits a potential for a catalyst in nitrogen fixation.[12] The $M(CO)_5N_2$ (*M*=Cr, Mo, W) complexes have been observed in the liquid xenon and low-temperature matrices.[13] The $Rh(CO)N_2$, $Rh^{II}(CO)(N_2)^{2+}$, and $Rh^{II}(CO)_2(N_2)^{2+}$ species have been produced from the reactions of nitrogen gas with rhodium carbonyls supported on dealuminated Y zeolite and an Al_2O_3 surface.[14,15]

Previous studies have shown that, with the aid of isotopic substitution, matrix isolation infrared spectroscopy, combined with density functional theory (DFT) calculation, is very powerful in investigating the spectrum, structure, and bonding of novel species and the related reaction mechanisms.[16,17] Recently, various metal carbonyls have been prepared in low-temperature matrices by codeposition of laser-ablated transition-metal and main-group-element atoms with CO.[8,9] Neon matrix investigations of the reaction of laser-ablated tantalum and niobium atoms with carbon monoxide molecules have characterized the $M(CO)_x$ (x=1–6) (*M*=Ta, Nb) molecules.[18] Similarly, some tantalum and niobium dinitrogen complexes have been identified in the argon matrix experiments.[19] In this paper, we report a study of the reactions of laser-ablated Ta and Nb atoms with CO and N_2 mixtures in excess neon. IR spectroscopy coupled with theoretical calculation provides evidence for the formation of the new carbonylmetal dinitrogen complexes, NN*M*CO (*M*=Ta, Nb), $(NN)_2$TaCO, and $NNTa(CO)_2$.

II. EXPERIMENTAL AND THEORETICAL METHODS

The experiments for laser ablation and matrix isolation infrared spectroscopy are similar to those previously reported.[20] Briefly, the Nd:yttrium aluminum garnet laser fundamental (1064 nm, 10 Hz repetition rate with 10 ns pulse width) was focused on the rotating Ta and Nb targets. The laser energy was varied from 5 to 25 mJ/pulse. The laser-ablated Ta and Nb atoms were codeposited with CO and N_2 mixtures in excess neon onto a CsI window cooled normally to 4 K by means of a closed-cycle helium refrigerator. CO (99.95%, Japan Fine Products), $^{13}C^{16}O$ (99%, $^{18}O<1\%$, ICON), $^{12}C^{18}O$ (99%, ICON), N_2 (99.95%, SUZUKI SHOKAN Co., Ltd.), $^{15}N_2$ (99.8%, SHOKO Co., Ltd.), and mixed isotopic samples were used to prepare the $CO/N_2/Ne$ mixtures. In general, matrix samples were deposited for 30–60 min with a typical rate of 2–4 mmol/h. After sample deposition, IR spectra were recorded on a BIO-RAD FTS-6000e spectrometer at 0.5 cm^{-1} resolution using a liquid nitrogen cooled HgCdTe (MCT) detector for the spectral range of 5000–400 cm^{-1}. Samples were annealed at different temperatures and subjected to broadband irradiation ($\lambda>250$ nm) using a high-pressure mercury arc lamp (Ushio, 100 W).

DFT calculations were performed to predict the structures and vibrational frequencies of the observed reaction

a)Author to whom correspondence should be addressed. Electronic mail: q.xu@aist.go.jp.

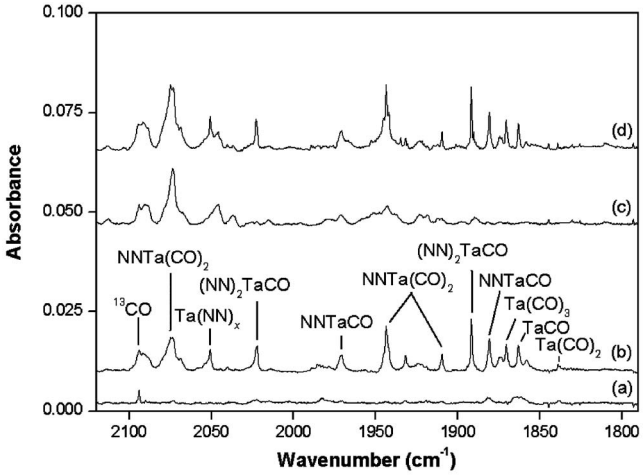

FIG. 1. Infrared spectra in the 2120–1790 cm^{-1} region from codeposition of laser-ablated Ta atoms with 0.1%CO+0.3%N_2 in Ne. (a) 40 min of sample deposition at 4 K, (b) after annealing to 10 K, (c) after 10 min of broadband irradiation, and (d) after annealing to 12 K.

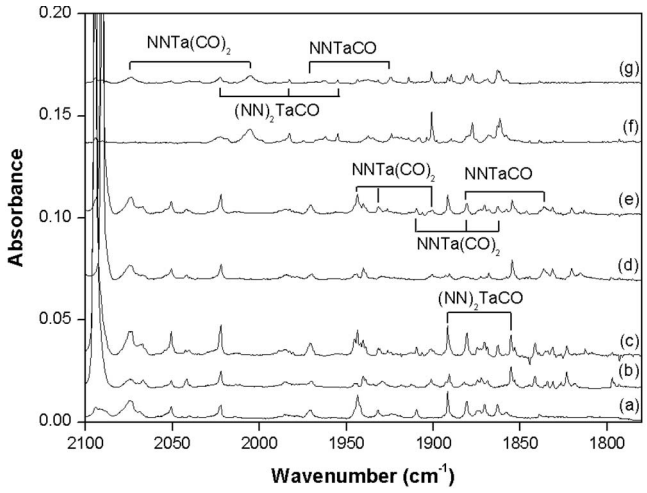

FIG. 2. Infrared spectra in the 2100–1780 cm^{-1} region for laser-ablated Ta atoms codeposited with isotopic CO/N_2 mixtures in Ne after annealing to 10 K. (a) 0.1%CO+0.3%N_2, (b) 0.1% ^{13}CO+0.3%N_2, (c) 0.1% ^{12}CO +0.1% ^{13}CO+0.3%N_2, (d) 0.1%C ^{18}O+0.3%N_2, (e) 0.1%C ^{16}O +0.1%C ^{18}O+0.3%N_2, (f) 0.1%CO+0.3% $^{15}N_2$, and (g) 0.1%CO +0.2% $^{14}N_2$+0.2% $^{15}N_2$.

products using the GAUSSIAN 03 program.[21] The BP86 density functional method was utilized,[22] which have been shown to provide vibrational frequencies close to the experimental values.[23–25] The 6-311+G(*d*) basis set was used for the C, O, and N atoms,[26] and the Los Alamos effective-core-potential plus double zeta (LANL2DZ) basis set was used for the Ta and Nb atoms.[27] All geometrical parameters were fully optimized and the harmonic vibrational frequencies were calculated with analytical second derivatives. Natural bond orbital[28] (NBO) approach was employed to elucidate the electron configurations and bonding characteristics. Trial calculations and recent investigations have shown that such computational methods can provide reliable information for metal complexes, such as infrared frequencies, relative absorption intensities, and isotopic shifts.[16–19,23–25]

III. RESULTS AND DISCUSSION

Experiments have been done for laser-ablated Ta and Nb atoms reactions with CO and N_2 mixtures in excess neon using low laser energy with different CO and N_2 concentrations. Typical infrared spectra for the products in the selected regions are illustrated in Figs. 1–4, and the absorption bands in different isotopic experiments are listed in Table I. Absorptions common to these experiments such as metal carbonyls, metal dinitrogen complexes, and ^{13}CO have been reported previously[18,19] and are not listed here. The stepwise annealing and photolysis behavior of the product absorptions is also shown in the figures and will be discussed below. Meanwhile, experiments have also been done for the codeposition of laser-ablated Ta and Nb atoms with separated CO and N_2 samples to confirm the new absorptions.

DFT calculations have been carried out for the possible isomers and electronic states of the potential product molecules. Figure 5 shows the ground state structures of the new products. The ground electronic states, point groups, vibrational frequencies, and intensities are listed in Table II. Table III reports a comparison of the observed and calculated isotopic frequency ratios for the N–N and C–O stretching modes of the novel products. The summary of electronic configurations, natural charge distributions, the TaCO bond angles and C–O stretching frequencies of tantalum monocarbonyl subunits in the series of complexes are listed in Table IV. Energetic analysis for possible reactions of Ta and Nb atoms with CO and N_2 is given in Table V. Molecular orbital depictions of the highest occupied molecular orbitals (HOMOs) and HOMO-1*s* of the new products are representatively illustrated in Fig. 6.

A. NNTaCO

In the Ta+CO+N_2 experiments, the absorptions at 1970.6 and 1880.7 cm^{-1} appear together after sample annealing, visibly decrease after broadband irradiation, and markedly recover after further annealing to higher temperature (Table I and Fig. 1). The lower band at 1880.7 cm^{-1}

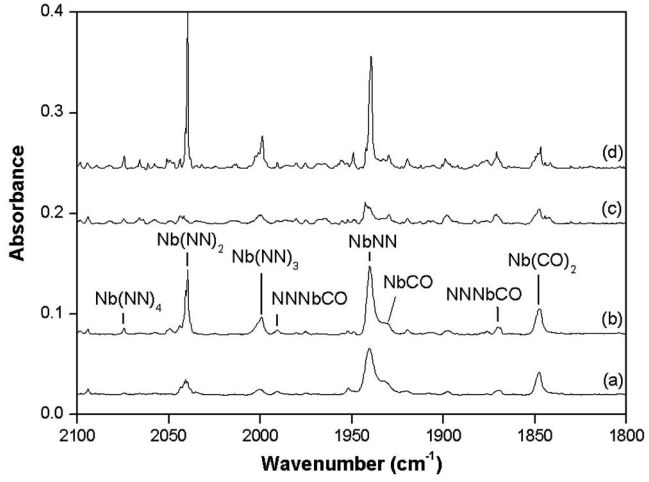

FIG. 3. Infrared spectra in the 2100–1800 cm^{-1} region from codeposition of laser-ablated Nb atoms with 0.15%CO+0.1%N_2 in Ne. (a) 40 min of sample deposition at 4 K, (b) after annealing to 8 K, (c) after 10 min of broadband irradiation, and (d) after annealing to 10 K.

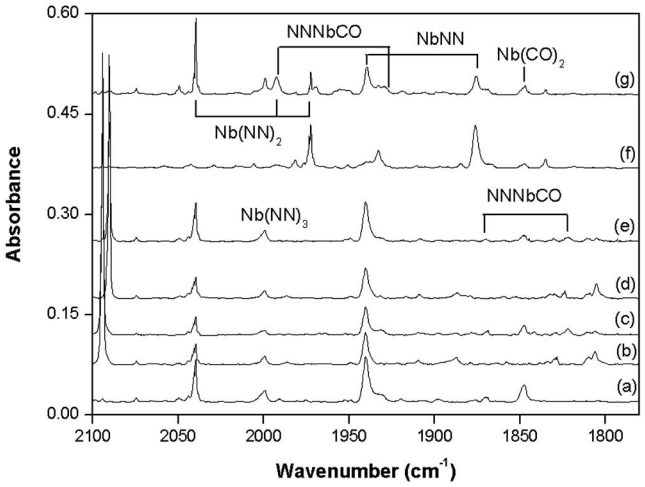

FIG. 4. Infrared spectra in the 2100–1780 cm^{-1} region for laser-ablated Nb atoms codeposited with isotopic CO/N_2 mixtures in Ne after annealing to 8 K. (a) 0.15%CO+0.1%N_2, (b) 0.15% ^{13}CO+0.1%N_2, (c) 0.1% ^{12}CO +0.1% ^{13}CO+0.1%N_2, (d) 0.15%C ^{18}O+0.1%N_2, (e) 0.1%C ^{16}O +0.1%C ^{18}O+0.1%N_2, (f) 0.15%CO+0.2% $^{15}N_2$, and (g) 0.2%CO +0.15% $^{14}N_2$+0.15% $^{15}N_2$.

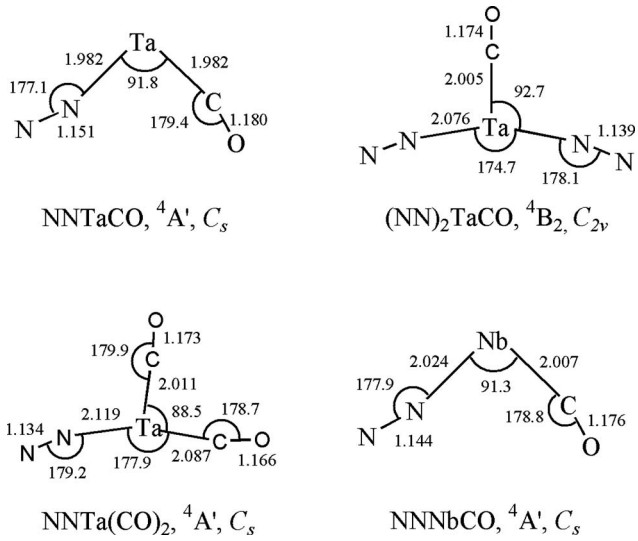

FIG. 5. Optimized structures (bond lengths in angstrom, bond angles in degree), electronic ground states, point groups of the new reaction products calculated at the BP86/6-311+G(*d*)-LANL2DZ level.

shifts to 1841.5 cm^{-1} with $^{13}C^{16}O$ and to 1836.5 cm^{-1} with $^{12}C^{18}O$, exhibiting isotopic frequency ratios ($^{12}C^{16}O/^{13}C^{16}O$: 1.0213; $^{12}C^{16}O/^{12}C^{18}O$: 1.0241) characteristic of C–O stretching vibrations. The mixed $^{12}C^{16}O$ + $^{13}C^{16}O$+N_2 (Fig. 2, trace c) and $^{12}C^{16}O$+ $^{12}C^{18}O$+N_2 (Fig. 2, trace e) isotopic spectra only provide the sum of pure isotopic bands, implying that one CO unit is involved in this mode.[29] This band is 15.5 cm^{-1} higher than the band for TaCO in a neon matrix.[18] Furthermore, the 1880.7 cm^{-1} band also shows a small shift with $^{15}N_2$ (19.1 cm^{-1}) (Table I and Fig. 2), suggesting that the N_2 unit is involved in this complex. The upper band at 1970.6 cm^{-1} shows very small shifts with $^{13}C^{16}O$ and $^{12}C^{18}O$ ($^{12}C^{16}O/^{13}C^{16}O$: 1.0004; $^{12}C^{16}O/^{12}C^{18}O$: 1.0005) but a large shift with $^{15}N_2$ ($^{14}N_2/^{15}N_2$: 1.0242), indicating that this mode is mainly due to a N–N stretching vibration. This band is 17.8 cm^{-1} higher than the N–N vibrational frequency of TaNN in an argon matrix.[19] The mixed CO+ $^{14}N_2$+ $^{15}N_2$ isotopic spectra (Fig. 2, trace g) only provide the sum of pure isotopic bands, which indicates only one N_2 unit is involved in the complex.[29] Accordingly, the absorptions at 1970.6 and 1880.7 cm^{-1} are assigned to the N–N and C–O stretching modes of NNTaCO, respectively.

DFT calculations have been performed for the NNTaCO complex to support the above assignment. The NNTaCO complex is predicted to have a $^4A'$ ground state with C_s symmetry (Table II and Fig. 5). The N–N and C–O stretching vibrational frequencies of the bent NNTaCO complex are calculated to be 1938.9 and 1849.7 cm^{-1} (Table II), respectively, which are in accord with the corresponding experimental values. For the C–O stretching mode of the bent NNTaCO complex, the calculated $^{12}C^{16}O/^{13}C^{16}O$, $^{12}C^{16}O/^{12}C^{18}O$, and $^{14}N/^{15}N$ isotopic frequency ratios of 1.0217, 1.0204, and 1.0101 (Table III) are consistent with the experimental observations, 1.0213, 1.0241, and 1.0103, respectively. The calculated $^{12}C^{16}O/^{13}C^{16}O$, $^{12}C^{16}O/^{12}C^{18}O$, and $^{14}N/^{15}N$ isotopic frequency ratios of the N–N stretching mode of the bent NNTaCO complex also agree with the experimental values (Table III).

TABLE I. IR absorptions (in cm^{-1}) of new species observed from reaction of laser-ablated Ta and Nb atoms with CO and N_2 mixtures in excess neon.

$CO+N_2$	$^{13}CO+N_2$	$C^{18}O+N_2$	$CO+^{15}N_2$	$R(^{12}CO/^{13}CO)$	$R(C^{16}O/C^{18}O)$	$R(^{14}N/^{15}N)$	Assignment
				Tantalum			
2074.0	2073.5	2073.8	2006.1	1.0002	1.0001	1.0339	$NNTa(CO)_2$
2022.2	2022.1	2022.0	1954.9	1.0001	1.0001	1.0344	$(NN)_2TaCO$
1970.6	1969.9	1969.7	1924.0	1.0004	1.0005	1.0242	NNTaCO
1943.6	1901.2	1900.6	1937.5	1.0223	1.0226	1.0031	$NNTa(CO)_2$
1909.6	1868.8	1863.0	1908.2	1.0218	1.0250	1.0007	$NNTa(CO)_2$
1891.7	1855.4	1854.7	1877.5	1.0196	1.0200	1.0076	$(NN)_2TaCO$
1880.7	1841.5	1836.5	1861.6	1.0213	1.0241	1.0103	NNTaCO
				Niobium			
1990.8	1986.3	1986.6	1923.1	1.0023	1.0021	1.0352	NNNbCO
1870.2	1828.2	1823.6	1868.7	1.0230	1.0256	1.0008	NNNbCO

TABLE II. Ground electronic states, point groups, vibrational frequencies (cm^{-1}), and intensities (km/mol) of the new products calculated at the BP86/6-311+G(*d*)-LANL2DZ level.

Species	Ground electronic state	Point group	Frequency (intensity, mode)
NNTaCO	$^4A'$	C_s	1938.9 (453, A'), 1849.7 (1123, A'), 514.2 (0.4, A'), 470.1 (4, A'), 433.2 (20, A'), 369.1 (1, A'), 335.4 (2, A''), 320.8 (2, A''), 85.6 (1, A')
$(NN)_2TaCO$	$^4B_2$	C_{2v}	2065.0 (5, A_1), 2005.8 (1750, B_2), 1885.7 (976, A_1), 509.2 (4, A_1), 485.4 (0.005, B_2), 452.4 (4, A_1), 399.3 (0.06, B_1), 389.2 (3, A_1), 361.8 (42, B_2), 328.7 (2, B_1), 328.6 (10, B_2), 287.3 (0, A_2), 80.7 (1, B_2), 73.6 (1, A_1), 51.4 (2, B_1)
$NNTa(CO)_2$	$^4A'$	C_s	2078.8 (347, A'), 1940.5 (1668, A'), 1886.2 (1010, A'), 539.9 (7, A'), 480.7 (0.4, A'), 452.0 (4, A'), 404.6 (10, A'), 398.7 (0.03, A''), 343.2 (21, A'), 329.2 (1, A''), 321.4 (20, A'), 279.8 (0.07, A''), 80.7 (1, A'), 65.6 (1, A'), 34 (2, A'')
NNNbCO	$^4A'$	C_s	1991.9 (517, A'), 1868.5 (1060, A'), 541.8 (0.3, A'), 460.9 (3, A'), 414.1 (17, A'), 345.6 (3, A'), 321.2 (5, A''), 303.3 (3, A''), 84.4 (1, A')

B. $(NN)_2TaCO$

In the Ta+CO+N_2 experiments, the sharp bands at 2022.2 and 1891.7 cm^{-1} appear together after sample annealing, markedly decrease after broadband irradiation, and recover after further annealing to higher temperature (Table I and Fig. 1). The lower band at 1891.7 cm^{-1} shifts to 1855.4 cm^{-1} with $^{13}C^{16}O$ and to 1854.7 cm^{-1} with $^{12}C^{18}O$, exhibiting isotopic frequency ratios ($^{12}C^{16}O/^{13}C^{16}O$: 1.0196; $^{12}C^{16}O/^{12}C^{18}O$: 1.0200) characteristic of C–O stretching vibrations. The mixed $^{12}C^{16}O+^{13}C^{16}O+N_2$ (Fig. 2, trace c) and $^{12}C^{16}O+^{12}C^{18}O+N_2$ (Fig. 2, trace e) isotopic spectra only provide the sum of pure isotopic bands, implying that one CO unit is involved in this mode.[29] This band is 26.5 cm^{-1} higher than the band for TaCO in solid neon.[18] Furthermore, the 1891.7 cm^{-1} band also shows a small shift with $^{15}N_2$ (Table I and Fig. 2), suggesting that the N_2 unit is involved in this complex. The upper band at 2022.2 cm^{-1} shows a large shift with $^{15}N_2$ ($^{14}N_2/^{15}N_2$: 1.0344), indicating that this mode is mainly due to a N–N stretching vibration. A triplet isotopic pattern is observed in the mixed CO+$^{14}N_2$+$^{15}N_2$ isotopic spectra (Fig. 2, trace g), which indicates two N_2 units are involved in the complex.[29] This band is 51.6 cm^{-1} higher than the N–N vibrational frequency of NNTaCO in present experiments. Accordingly, the absorptions at 2022.2 and 1891.7 cm^{-1} are assigned to the asymmetric N–N and C–O stretching modes of $(NN)_2TaCO$, respectively.

The $(NN)_2TaCO$ complex is predicted to have a $^4B_2$ ground state with C_{2v} symmetry (Table II and Fig. 5). The symmetric and asymmetric N–N and C–O stretching frequencies of the $(NN)_2TaCO$ species are calculated to be 2065.0, 2005.8, and 1885.7 cm^{-1} (Table II), respectively. The intensity of the symmetric N–N stretching vibration in $(NN)_2TaCO$ is predicted to be about 1/350 that of the asymmetric N–N stretching vibration (Table III), which is consistent with the absence of the symmetric N–N stretching vibration of the $(NN)_2TaCO$ complex from the present experiments. The calculated $^{12}C^{16}O/^{13}C^{16}O$, $^{12}C^{16}O/^{12}C^{18}O$, and $^{14}N/^{15}N$ isotopic frequency ratios of the asymmetric N–N and C–O stretching vibrations are consistent with the experimental values (Table III), respectively, which support the identification of the $(NN)_2TaCO$ complex.

C. $NNTa(CO)_2$

In the Ta+CO+N_2 experiments, new bands at 2074.0, 1943.6, and 1909.6 cm^{-1} exhibit the same behavior of depo-

TABLE III. Comparison of observed and calculated IR frequency ratios for the new products.

	Frequency (cm^{-1})			$R(^{12}CO/^{13}CO)$		$R(C^{16}O/C^{18}O)$		$R(^{14}N/^{15}N)$	
Species	Obs.	Calc.	Mode	Obs.	Calc.	Obs.	Calc.	Obs.	Calc.
NNTaCO	1970.6	1938.9	ν_{N-N}	1.0004	1.0023	1.0005	1.0021	1.0242	1.0247
	1880.7	1849.7	ν_{C-O}	1.0213	1.0217	1.0241	1.0204	1.0103	1.0101
$(NN)_2TaCO$	2022.2	2005.8	ν_{N-N}	1.0001	1.0000	1.0001	1.0000	1.0344	1.0350
	1891.7	1885.7	ν_{C-O}	1.0196	1.0231	1.0200	1.0221	1.0076	1.0024
$NNTa(CO)_2$	2074.0	2078.8	ν_{N-N}	1.0002	1.0018	1.0001	1.0015	1.0339	1.0293
	1943.6	1940.5	ν_{C-O}	1.0223	1.0220	1.0226	1.0216	1.0031	1.0054
	1909.6	1886.2	ν_{C-O}	1.0218	1.0238	1.0250	1.0231	1.0007	1.0001
NNNbCO	1990.8	1991.9	ν_{N-N}	1.0023	1.0013	1.0021	1.0012	1.0352	1.0303
	1870.2	1868.5	ν_{C-O}	1.0230	1.0226	1.0256	1.0219	1.0008	1.0045

TABLE IV. Summary of the electronic configurations, natural charges, TaCO angles (deg), and C–O stretching frequencies (cm^{-1}) in the $(NN)_xTa(CO)_y$ molecules.

Species	Ta electronic configuration	C electronic configuration	q_{Ta}	q_C	$\angle MCO$	$\nu_{C\text{-}O}$ Obs.	$\nu_{C\text{-}O}$ Calc.
$TaCO(^6\Sigma^+)$	$6s^{0.95}5d^{3.78}$	$2s^{1.30}2p^{2.49}$	0.280	0.151	180.0	1863.0	1900.5
$NNTaCO(C_s)$	$6s^{0.79}5d^{3.59}$	$2s^{1.25}2p^{2.53}$	0.636	0.172	179.4	1880.7	1849.7
$(NN)_2TaCO(C_{2v})$	$6s^{0.66}5d^{3.68}$	$2s^{1.24}2p^{2.46}$	0.676	0.253	180.0	1891.7	1885.7
$NNTa(CO)_2(C_s)$	$6s^{0.69}5d^{3.80}$	$2s^{1.33}2p^{2.37}$	0.534	0.247	178.7	1943.6	1940.5
		$2s^{1.24}2p^{2.45}$		0.264	179.9	1909.6	1886.2

sition, annealing, and broadband irradiation experiments, suggesting that they are due to different vibrational modes of the same molecule (Table I and Fig. 1). The 1943.6 and 1909.6 cm^{-1} bands shift to 1901.2 and 1868.8 cm^{-1} with $^{13}C^{16}O$, and to 1900.6 and 1863.0 cm^{-1} with $^{12}C^{18}O$, respectively, exhibiting isotopic frequency ratios characteristic of C–O stretching vibrations. The mixed $^{12}C^{16}O+^{13}C^{16}O+N_2$ (Fig. 2, trace c) and $^{12}C^{16}O+^{12}C^{18}O+N_2$ (Fig. 2, trace e) isotopic spectra show a triplet isotopic pattern, respectively, implying that two CO units are involved in this mode.[29] Furthermore, the 1943.6 and 1909.6 cm^{-1} bands also show a small shift with $^{15}N_2$ (Table I and Fig. 2), suggesting that the N_2 unit is involved in this complex. The 1943.6 and 1909.6 cm^{-1} bands are 25.3 and 71.0 cm^{-1} higher than the symmetric and asymmetric C–O vibrational frequencies of bent $Ta(CO)_2$ in a neon matrix, respectively.[19] The upper band at 2074.0 cm^{-1} shows a large shift with $^{15}N_2$ ($^{14}N_2/^{15}N_2$: 1.0339), indicating that this mode is mainly due to a N–N stretching vibration. The mixed $CO+^{14}N_2+^{15}N_2$ isotopic spectra (Fig. 2, trace g) only provide the sum of pure isotopic bands, which indicates only one N_2 unit is involved in the complex.[29] This band is 121.2, 103.4, and 51.8 cm^{-1}, respectively, higher than the N–N vibrational frequency of TaNN in solid argon,[19] and those of NNTaCO and $(NN)_2TaCO$ in solid neon in the present experiments. Accordingly, the absorptions at 2074.0, 1943.6, and 1909.6 cm^{-1} are assigned to the N–N, symmetric C–O, and asymmetric C–O stretching vibrations of $NNTa(CO)_2$, respectively.

TABLE V. Energetics for possible reactions of Ta and Nb atoms with CO and N_2 calculated at the BP86/6-311+G(*d*)-LANL2DZ level.

No.	Reaction	Reaction energy[a] (kcal/mol)
1	$Ta(^4F)+CO(^1\Sigma^+)\rightarrow TaCO(^6\Sigma^+)$	−41.4
2	$Ta(^4F)+N_2(^1\Sigma_g^+)\rightarrow TaNN(^6\Sigma^+)$	−26.4
3	$Nb(^6D)+CO(^1\Sigma^+)\rightarrow NbCO(^6\Sigma^+)$	−44.6
4	$Nb(^6D)+N_2(^1\Sigma_g^+)\rightarrow NbNN(^6\Sigma^+)$	−30.9
5	$TaNN(^6\Sigma^+)+CO(^1\Sigma^+)\rightarrow NNTaCO(C_s)$	−50.0
6	$TaCO(^6\Sigma^+)+N_2(^1\Sigma_g^+)\rightarrow NNTaCO(C_s)$	−35.0
7	$NbNN(^6\Sigma^+)+CO(^1\Sigma^+)\rightarrow NNNbCO(C_s)$	−41.2
8	$NbCO(^6\Sigma^+)+N_2(^1\Sigma_g^+)\rightarrow NNNbCO(C_s)$	−27.5
9	$Ta(NN)_2(^6A_1)+CO(^1\Sigma^+)\rightarrow (NN)_2TaCO(C_{2v})$	−53.1
10	$NNTaCO(C_s)+N_2(^1\Sigma_g^+)\rightarrow (NN)_2TaCO(C_{2v})$	−31.4
11	$NNTaCO(C_s)+CO(^1\Sigma^+)\rightarrow NNTa(CO)_2(C_s)$	−46.8
12	$Ta(CO)_2(^4B_2)+N_2(^1\Sigma_g^+)\rightarrow NNTa(CO)_2(C_s)$	−24.9

[a]A negative value of energy denotes that the reaction is exothermic.

$NNTa(CO)_2$ is predicted to have a C_s symmetry (Fig. 5) with a $^4A'$ ground state (Table II). The N–N, symmetric C–O, and asymmetric C–O stretching vibrations are calculated to be 2078.8, 1940.5, and 1886.2 cm^{-1} (Table III), respectively, which are consistent with the observed frequencies. The calculated $^{12}C^{16}O/^{13}C^{16}O$, $^{12}C^{16}O/^{12}C^{18}O$, and $^{14}N/^{15}N$ isotopic frequency ratios of N–N, symmetric C–O, and asymmetric C–O stretching vibrations are in accord with the experimental values (Table III), respectively. These overall agreements support the above assignment of the $NNTa(CO)_2$ complex from the matrix spectra.

D. NNNbCO

In the $Nb+CO+N_2$ experiments, weak absorptions at 1990.8 and 1870.2 cm^{-1} appear together during sample deposition, slightly increase upon sample annealing, slightly decrease after broadband irradiation, and slightly increase after further annealing to 10 K (Table I and Fig. 3). The 1870.2 cm^{-1} band shows large shifts (42.0, and 46.6 cm^{-1}) with $^{13}C^{16}O$ and $^{12}C^{18}O$, respectively, but only a small shift (1.5 cm^{-1}) with $^{15}N_2$. The $^{12}C^{16}O/^{13}C^{16}O$ isotopic ratio of 1.0230, $^{12}C^{16}O/^{12}C^{18}O$ isotopic ratio of 1.0256 and $^{14}N/^{15}N$ isotopic ratio of 1.0008 suggest that this band is due to a terminal C–O stretching vibration with small coupling to nitrogen. This band is 61.8 cm^{-1} lower than the C–O stretch-

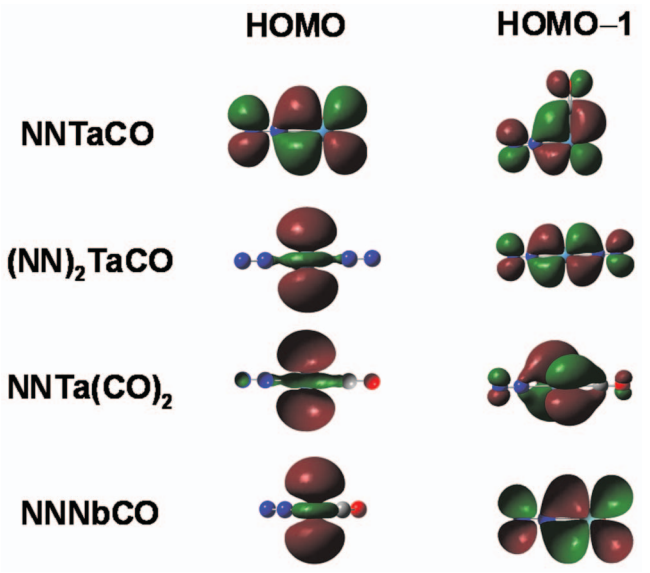

FIG. 6. Molecular orbital depictions of the HOMOs and HOMO-1*s* of the new products.

ing vibration frequency for NbCO and 23.0 cm^{-1} higher than the antisymmetric C–O stretching vibration frequency for $Nb(CO)_2$ in a neon matrix.[18] The 1990.8 cm^{-1} band exhibits small shifts (4.5 and 4.2 cm^{-1}) with $^{13}C^{16}O$ and $^{13}C^{18}O$, respectively, but a large shift (67.7 cm^{-1}) with $^{15}N_2$. The $^{14}N/^{15}N$ isotopic ratio of 1.0352 indicates that this band is mainly due to a terminal N–N stretching vibration. This band is 76.3 cm^{-1} higher than the N–N vibrational frequency of NbNN in solid argon.[19] In the mixed $^{12}C^{16}O+^{13}C^{16}O+N_2$, $^{12}C^{16}O+^{12}C^{18}O+N_2$, and $CO+^{14}N_2+^{15}N_2$ experiments (Fig. 4), the sum of pure isotopic bands are observed, indicating only one CO and N_2 unit are involved in the complex, respectively. Therefore, the absorptions at 1990.8 and 1870.2 cm^{-1} are assigned to the N–N and C–O stretching vibrations of NNNbCO, respectively.

The assignment is confirmed by DFT calculations summarized in Table II. The C–O stretching frequency is calculated at 1868.5 cm^{-1}, only 1.7 cm^{-1} lower than the observed value. The calculated N–N stretching frequency (1991.9 cm^{-1}) also agrees with the observed value. For the C–O stretching mode, the calculated $^{12}C^{16}O/^{13}C^{16}O$, $^{12}C^{16}O/^{12}C^{18}O$, and $^{14}N/^{15}N$ isotopic frequency ratios of 1.0226, 1.0219, and 1.0045 (Table III) are consistent with the experimental observations, 1.0230, 1.0256, and 1.0008, respectively. Similar results have also been obtained for the N–N stretching mode of the NNNbCO complex (Table III).

E. Bonding considerations

It is interesting to compare the electronic configurations, natural charge distributions, and C–O stretching frequencies of tantalum monocarbonyl subunits in the series of complexes in Table IV. The TaCO molecule is calculated to be linear with a $^6\Sigma^+$ ground state calculated at the BP86/6-311+G(*d*)-LanL2DZ. However, the Ta–CO bond is weakened upon coordination of N_2 ligands. As a result the C–O stretching vibrations are increased as the natural charge distributions of tantalum atoms become more positive. In TaCO, σ donation from the 5σ molecular orbital of CO contributes to the unoccupied Ta orbital of σ symmetry ($d\sigma$), while the π back donation is from the $5d\pi$(Ta) orbital to the empty antibonding orbital ($2\pi^*$) of CO. The $5d\pi$(Ta) orbital is oriented to Ta–C bond with optimized $\pi-$overlap. However, the $5d\pi(\mathrm{Ta})-2\pi^*(\mathrm{CO})$ interaction is reduced since both of the charge distribution of Ta atom and orientation of the $5d\pi$(Ta) orbital are strongly perturbed by Ta–N bonding. Therefore, the bent TaCO subunits are obtained in the NNTaCO and $NNTa(CO)_2$ complexes except for the C_{2v} symmetry $(NN)_2TaCO$. In addition, the π back donation is reduced from more positive Ta centers, and more electron-poor Ta centers produce higher C–O (N–N) stretching vibrations in the series of tantalum carbonyl dinitrogen complexes. Therefore the C–O and N–N frequencies increase with the total number of ligands (Table III). Similar features are also predicted for the niobium and other metal higher carbonyl dinitrogen complexes.

As illustrated in Fig. 6, the HOMO in NNTaCO is the M–N π bonding orbital and mainly results from the contributions between Ta 5*d* and N 2*p* atomic orbitals, whereas the HOMO in NNNbCO is largely Nb 4*d* in character and is nonbonding. The HOMOs of $(NN)_2TaCO$ and $NNTa(CO)_2$ are largely Ta 5*d* in character and are nonbonding. In addition, the HOMO-1*s* in NNTaCO and $NNTa(CO)_2$ are π-type bonds, which comprise the $d\pi(\mathrm{Ta})$-$\pi^*(\mathrm{CO})$ and $d\pi(\mathrm{Ta})$-$\pi^*(N_2)$ back bonding, leading to the weakening of the C–O and N–N bonds. Similar to the HOMO of NNTaCO, the HOMO-1*s* in $(NN)_2TaCO$ and NNNbCO are the M–N π bonding orbitals, which are responsible for the stability of these carbonylmetal dinitrogen complexes.

F. Reaction mechanisms

On the basis of the behavior of sample annealing and irradiation, together with the observed species and calculated stable isomers, the plausible reaction mechanisms can be proposed as follows. Under the present experimental conditions, laser-ablated tantalum and niobium atoms react with CO and N_2 mixtures in the excess neon matrices to produce carbonylmetal dinitrogen species as well as metal carbonyls and metal dinitrogen complexes. Binary metal carbonyls and metal dinitrogen species have been prepared by reactions of Ta and Nb atoms with CO and N_2 separately, and identified by infrared spectroscopy.[18,19]

Table V presents the energetics for possible reactions of Ta and Nb atoms with CO and N_2 mixtures calculated at the BP86/6-311+G(*d*)-LanL2DZ. Reactions 1 and 2 are exothermic by 41.4 and 26.4 kcal/mol, respectively. In contrast to the formation of TaNN species (reaction 2), energy changes for the analogous carbonyl TaCO (reactions 1) are more exothermic, hence the carbonyls are more stable, based on the conventional wisdom that CO is a strong σ donor and π acceptor than the isoelectronic N_2 molecules.[30] In our present $Ta+CO+N_2$ experiments (Fig. 1), TaNN was not observed after matrix deposition and annealing, whereas the TaCO species was detected after deposition and annealing, indicating that Ta prefers the reaction with CO to the reaction with N_2, as supported by the calculated reaction energies (Table V). However, in the $Nb+CO+N_2$ experiments (Fig. 3), NbNN was observed after deposition as well as TaCO species, indicating that the reactivity of Nb to N_2 is comparable to that of CO. The formation is exothermic by 44.6 kcal/mol for NbCO (reactions 3) and by 30.9 kcal/mol for NbNN (reaction 4).

The carbonylmetal dinitrogen complexes may be formed from the reactions of metal carbonyls with N_2 or metal dinitrogen complexes with CO (Table V, reactions 5–12). Furthermore, the reactions of metal dinitrogen complexes with CO are calculated to be exothermic by 50.0 kcal/mol for Ta (reaction 5) and 41.2 kcal/mol for Nb (reaction 7) whereas the reactions of metal carbonyls with N_2 are calculated to be exothermic by 35.0 kcal/mol for Ta (reaction 6) and 27.5 kcal/mol for Nb (reaction 8), respectively. The NNTaCO molecule is mainly produced from reaction 6 during annealing. Although reaction 5 is more exothermic, the yield of TaNN is limited and not observed in the present neon matrix (Fig. 1). As for the reaction of Nb with CO and N_2 mixtures, the NNNbCO may be produced from both reactions 7 and 8.

The $(NN)_2TaCO$ and $NNTa(CO)_2$ complexes are produced on sample annealing, increased markedly on further annealing and became the dominant products, but the niobium counterparts are absent from the present matrix experiments. The reaction of $Ta(NN)_2$ with CO is calculated to be exothermic by 53.1 kcal/mol (reaction 9) whereas the reaction of NNTaCO with N_2 is calculated to be exothermic by 31.4 kcal/mol (reaction 10). The $(NN)_2TaCO$ molecule is mainly produced from reaction 10 during annealing. Although reaction 9 is more exothermic, the yield of $Ta(NN)_2$ as well as TaNN is limited and not observed in the present neon matrix (Fig. 1). As for the formation of $NNTa(CO)_2$, reactions 11 and 12 are exothermic by 46.8 and 24.9 kcal/mol, respectively. Reactions 11 and 12 may be parallel for the formation of $NNTa(CO)_2$. However, in the Nb+CO $+N_2$ experiments, it is possible that the higher niobium dinitrogen complexes may be formed from the reactions of primary NNNbCO with CO or N_2. The yield of NNNbCO is limited in the present experiments (Fig. 3). Therefore $(NN)_2NbCO$ and $NNNb(CO)_2$ are absent from the present $Nb+CO+N_2$ experiments.

IV. CONCLUSIONS

Reactions of laser-ablated Ta and Nb atoms with CO and N_2 mixtures in excess neon have been studied using matrix isolation infrared spectroscopy. Besides the metal carbonyls and dinitrogen complexes, the carbonylmetal dinitrogen complexes, NN*M*CO (*M*=Ta, Nb), $(NN)_2TaCO$, and $NNTa(CO)_2$, are formed during sample deposition or after annealing and are characterized using infrared spectroscopy on the basis of the results of the isotopic substitution and mixed isotopic splitting patterns. DFT calculations have been performed on these complexes. The identifications of these carbonylmetal dinitrogen complexes are confirmed by the overall agreement between the experimental and calculated vibrational frequencies, relative absorption intensities, and isotopic shifts.

ACKNOWLEDGMENTS

This work was supported by the AIST and a Grant-in-Aid for Scientific Research (B) (Grant No. 17350012) from the Ministry of Education, Culture, Sports, Science and Technology (MEXT) of Japan. Z.-H.L. acknowledges the JASSO and the Kobe University for Honors Scholarship.

[1] *Advanced Inorganic Chemistry*, edited by F. A. Cotton, G. Wilkinson, C. A. Murillo, and M. Bochmann (Wiley, New York, 1999).
[2] E. L. Muetterties and J. Stein, Chem. Rev. (Washington, D.C.) **79**, 479 (1979).
[3] J. B. Howard and D. C. Rees, Chem. Rev. (Washington, D.C.) **96**, 2965 (1996).
[4] N. K. Brugess and D. J. Lowe, Chem. Rev. (Washington, D.C.) **96**, 2983 (1996).
[5] J. A. Pool, E. Lobkovsky, and P. J. Chirik, Nature (London) **427**, 527 (2004).
[6] L. Mond, C. Langer, and F. Quincke, J. Chem. Soc. 749 (1890).
[7] A. D. Allen and C. V. Senoff, J. Chem. Soc. Chem. Commun. 621 (1965).
[8] M. F. Zhou, L. Andrews, and C. W. Bauschlicher, Jr., Chem. Rev. (Washington, D.C.) **101**, 1931 (2001).
[9] H. J. Himmel, A. J. Downs, and T. M. Greene, Chem. Rev. (Washington, D.C.) **102**, 4191 (2002).
[10] H. J. Himmel and M. Reiher, Angew. Chem., Int. Ed. **45**, 6264 (2006).
[11] D. Sellmann, Angew. Chem., Int. Ed. Engl. **10**, 919 (1971).
[12] D. Sellmann, Angew. Chem., Int. Ed. Engl. **11**, 534 (1972).
[13] J. J. Turner, M. B. Simpson, M. Poliakoff, W. B. Maier, and M. A. Graham, Inorg. Chem. **22**, 911 (1983); J. K. Burdett, A. J. Downs, G. P. Gaskill, M. A. Graham, J. J. Turner, and R. F. Turner, *ibid.* **17**, 523 (1978).
[14] E. A. Wovchko and J. T. Yates, Jr., J. Am. Chem. Soc. **118**, 10250 (1996).
[15] H. Miessner, J. Chem. Soc., Chem. Commun. 927 (1994); H. Miessner and K. Richter, J. Mol. Catal. Chem. **146**, 107 (1999).
[16] L. Andrews and A. Citra, Chem. Rev. (Washington, D.C.) **102**, 885 (2002); J. Li, B. E. Bursten, B. Liang, and L. Andrews, Science **295**, 2242 (2002); L. Andrews and X. Wang, *ibid.* **299**, 2049 (2003); X. Wang and L. Andrews, J. Am. Chem. Soc. **130**, 6766 (2008).
[17] M. F. Zhou, N. Tsumori, Z. Li, K. Fan, L. Andrews, and Q. Xu, J. Am. Chem. Soc. **124**, 12936 (2002); M. F. Zhou, Q. Xu, Z. Wang, and P. v. R. Schleyer, *ibid.* **124**, 14854 (2002); L. Jiang and Q. Xu, *ibid.* **127**, 42 (2005); Q. Xu, L. Jiang, and N. Tsumori, Angew. Chem., Int. Ed. **44**, 4338 (2005); L. Jiang and Q. Xu, J. Am. Chem. Soc. **127**, 8906 (2005).
[18] M. F. Zhou and L. Andrews, J. Phys. Chem. A **103**, 7785 (1999).
[19] M. F. Zhou and L. Andrews, J. Phys. Chem. A **102**, 9061 (1998).
[20] T. R. Burkholder and L. Andrews, J. Chem. Phys. **95**, 8697 (1991); P. Hassanzadeh and L. Andrews, *ibid.* **96**, 9177 (1992); L. Jiang and Q. Xu, *ibid.* **122**, 034505 (2005).
[21] M. J. Frisch, G. W. Trucks, H. B. Schlegel *et al.*, GAUSSIAN 03, revision B.04, Gaussian, Inc., Pittsburgh, PA, 2003.
[22] J. P. Perdew, Phys. Rev. B **33**, 8822 (1986); A. D. Becke, J. Chem. Phys. **98**, 5648 (1993).
[23] L. Jiang and Q. Xu, J. Chem. Phys. **128**, 124317 (2008).
[24] X. Feng, J. Gu, Y. Xie, R. B. King, and H. F. Schaefer, J. Chem. Theory Comput. **3**, 1580 (2007).
[25] S. Zhao, Z. H. Li, W. N. Wang, Z. P. Liu, K. N. Fan, Y. Xie, and H. F. Schaefer, J. Chem. Phys. **124**, 184102 (2006).
[26] A. D. McLean and G. S. Chandler, J. Chem. Phys. **72**, 5639 (1980); R. Krishnan, J. S. Binkley, R. Seeger, and J. A. Pople, *ibid.* **72**, 650 (1980); M. J. Frisch, J. A. Pople, and J. S. Binkley, *ibid.* **80**, 3265 (1984).
[27] P. J. Hay and W. R. Wadt, J. Chem. Phys. **82**, 299 (1985).
[28] E. D. Glendening, A. E. Reed, J. E. Carpenter, and F. Weinhold, NBO, version 3.1, University of Wisconsin, Madison, WI, 1995.
[29] J. H. Darling and J. S. Ogden, J. Chem. Soc. Dalton Trans. 2496 (1972).
[30] P. Pelikan and R. Boca, Coord. Chem. Rev. **55**, 55 (1984).